Supplementary Materials

Structure of *Mycobacterium tuberculosis* Cya, an evolutionary ancestor of the mammalian membrane adenylyl cyclases

Ved Mehta, Basavraj Khanppnavar, Dina Schuster, Irene Vercellino, Angela Kosturanova, Tarun Iype, Sasa Stefanic, Paola Picotti and Volodymyr M. Korkhov

Materials and Methods

Protein expression and purification

Expression and purification of the full-length Cya. Cya cloned into a vector with an N-terminal strep tag and a 3C cleavage tag was expressed in *E. coli* BL21(DE3)RIPL cells grown in TB medium. Protein expression was induced when at OD_{600} of 3.0 using 0.3 mM IPTG. After 3 hours of induction the cells were harvested. The membranes were prepared using cells lysis by three passes in Emusiflex high pressure homogenizer in a buffer containing 50 mM Tris pH 7.5, 200 mM NaCl, 5 μg/ml DNase and 1 mM PMSF. Lysed cells were centrifuged at 12000 rpm using a Ti45 rotor for 30 mins. The resulting supernatant was spun down by ultracentrifugation using Ti45 rotor at 40000 rpm for 1 hour, re-suspended in a buffer containing 50 mM Tris pH 7.5 and 200 mM NaCl and ultracentrifuged again. The resulting membrane pellet was resuspended in the same buffer, flash-frozen and stored at -80°C until purification.

For purification, the membranes were thawed and resuspended in a buffer containing 50 mM Tris pH 7.5, 200 mM NaCl, 10% glycerol and 1% sol-grade dodecylmaltoside (DDM, Anatrace), mixed at 4˚C for 1 hour and ultracentrifuged. The supernatant was incubated with Strep-tactin superflow resin for 1 hour at 4˚C. The resin was washed with a volume 25 times that of the resin bed of a buffer containing 0.1% digitonin and the eluted with 5 mM desthiobiotin. The eluted protein was concentrated and injected onto Superose 6 Increase column pre-equilibrated with a buffer containing 50 mM Tris pH 7.5, 200 mM NaCl 0.1% digitonin and 10% glycerol. For Cryo-EM samples glycerol was omitted during size exclusion chromatography step.

Cya-SOL expression and purification. Cya-SOL construct was generated by cloning the sequence encoding the Cya residues 203-433 into a vector with an N-terminal 10xHis tag followed by a 3C cleavage site. The construct was expressed in *E. coli* BL21(DE3)RIPL cells grown in TB medium. Expression was carried out under conditions similar to those used for expression of the full-length protein, with a 5-hour induction at 20˚C. The cells were collected by centrifugation, lysed and the cleared lysate was incubated with Ni-NTA resin for 1 hour. The resin was washed with a volume 15 times the resin bed volumne of wash buffer containing 50 mM Tris pH 7.5, 200 mM NaCl, 10% glycerol and 20 mM imidazole, followed by an additional wash step with a volume of 25 times the volume of the resin bed volume with a buffer containing 50 mM imidazole. The protein was eluted with a buffer containing 250 mM imidazole, concentrated and desalted using a GE PD-10 Sephadex G-25 desalting column. The protein was mixed with 3C protease (1/50 w/w) and incubated at 4˚C overnight. The protein was passed through pre-equilibrated Ni-NTA resin to remove the 3C protease and purified by SEC using Superdex 200 Increase column.

Nanobody library generation and selections

To generate desired immune response in heavy chain-only IgG subclass, an alpaca was immunized four times in two-week intervals, each time with 200 μg purified Rv1625c in PBS containing 0.02% (w/v) β-DDM. The antigen was mixed in a 1:1 (v/v) ratio with GERBU Fama adjuvant (GERBU Biotechnik GmbH, Heidelberg, Germany) and injected subcutaneously in 100 μL aliquots into the shoulder and neck region. Immunizations of alpacas were approved by the Cantonal Veterinary Office in Zurich, Switzerland (animal experiment licence nr. 172/2014). One week after the last injection, 60 mL of blood was collected from jugular vein for isolation of lymphocytes (Ficoll-Paque® PLUS, GE Healthcare Life Sciences, and Leucosep tubes, Greiner). Approx. 50 mio. cells were used to isolate mRNA (RNeasy Mini Kit, Qiagen) that was reverse transcribed into cDNA (AffinityScript, Agilent, US) using the gene specific primer. The VhH (nanobody) repertoire was amplified by PCR and phage library was generated

by fragment exchange cloning [Geertsma, 2011] into a PmlI-linearized pDX phagemid vector. The resulting VhH-phage library (size 4.5 e6) was screened by biopanning against the immobilized target. For that purpose VI23.60 containing Strep-tag® was immobilized on the Strep-Tactin® coated microplate (IBA Lifesciences GmbH, Germany) and three rounds of selection were performed. 195 single clones from the enriched nanobody library were induced to express polyhistidine-tagged soluble nanobodies in the bacterial periplasm and analysed by ELISA for binding to the target. 96 ELISA-positive clones were Sanger sequenced and grouped in 17 families according to their CDR3 length and sequence (*22*).

Nanobody expression and purification

Nanobody NB4 was expressed in BL21(DE3)RIPL cells in TB medium supplemented with 2 mM magnesium chloride and 0.1% glucose by induction at an OD_{600} of 0.7 using 1 mM IPTG at 26°C for 16 hours. The periplasmic fraction was isolated by resuspending the cell pellet in 2.5x w/v cold TES buffer (200 mM Tris pH 8.0, 0.5 mM EDTA and 0.5 mM sucrose and 1 mM PMSF) for 45 mins, followed by an overnight incubation with twice the amount of a 4-fold diluted TES buffer. The suspension was spun down and the supernatant was used for protein purification with Ni-NTA resin, following the same procedure as that used for Cya-SOL. The eluted nanobody was concentrated and further purified using SEC with a Superdex 200 Increase column.

Adenylyl cyclase activity assay

Adenylyl cyclase activity assays were performed as described previously (*17*). In brief, the assay was carried out in a reaction volume of 200 µl with 50mM Tris pH 8.0, 200 mM NaCl, 5 mM $MgCl_2$ 5 mM $MnCl_2$ and 0.1% digitonin. For determination of K_m, ATP concentration was varied from 0 to 1000 mM in presence of 10 nM [^{3}H]ATP (PerkinElmer). The reaction was initiated by adding ATP to the reaction solution containing 0.005 mg/ml Cya, 0.0075 mg/ml NB4, followed by an incubation for 10 min at 30˚C. The reaction was stopped by incubating the reaction mixture at 95˚C for 4 minutes and by addition of 20 µl of 2.2 M HCl. The stopped reactions were applied to 1.3 g of aluminum oxide in disposable columns. The cAMP was eluted with 4 ml of 100 mM ammonium acetate into scintillation vials and mixed with 12 ml scintillation liquid (Ultima Gold). The amount of radioactive cAMP was measured using a liquid scintillation counter. The activity assays for Cya-SOL were performed identically, using 0.08 mg/ml Cya-SOL in an assay.

Isothermal titration calorimetry

The isothermal titration calorimetry (ITC) experiments were performed using a Microcal ITC200 instrument with cell temperature maintained at 25˚C and with stirring set to 750 RPM. In total, 15 injections were performed per experiment with each injection set at 2 µl and a pre-injection volume of 0.8 µl. Cya-SOL was kept in the cell at a concentration of 30 µM and NB4 was kept in the syringe at 300 µM. All ITC measurements were performed in triplicates. The results were analyzed using sedphat and NITPIC. The figures describing the ITC results were generated using GUSSI (*38*).

Protein thermal unfolding

Protein thermal stability was measured using nanoDSF on a Prometheus panta instrument (NanoTemper) (*39*). The protein was measured at 0.5 mg/ml concentration in a buffer containing 50mM Tris pH 7.5, 200 mM NaCl and 0.1% digitonin, using NT.48 capillaries. For samples with ligand, 1mM

ATPαS and 5 mM $MgCl_2$ was added and allowed to incubate at RT for 10 minutes. The samples were spun at 13000 g on a tabletop centrifuge for 1 minute before measuring. Thermal unfolding experiments were carried out at a temperature increment of 1˚C/min in triplicates. Tm was calculated as the first derivative of intrinsic protein emission ratio at 350 nM and 330nM using PR.Panta analysis software.

Cryo-EM sample preparation

For Cryo-EM sample preparation, freshly purified full-length Cya in 0.1% digitonin was concentrated and mixed with NB4 at a molar ratio of 1:1.5. Additionally, 5 mM $MnCl_2$ and 0.5 mM MANT-GTP were added and the mixtures were incubated on ice for 30 minutes. The final concentration of Cya was 5-6 mg/ml. An aliquot of 3.5 µl of sample was placed on the glow-discharged cryo-EM grid (Quantifoil R1.2/1.3 or Quantifoil R2/1), blotted and plunge-frozen in liquid ethane using a Mark VI Vitrobot instrument maintained at 100% humidity with blot force 20 and blot time of 3 seconds. The grids were cryo-transferred for storage in liquid nitrogen.

Cryo-EM data acquisition and image analysis

The cryo-EM data were obtained at the SCOPEM facility at ETHZ using a 300 kV Titan Krios electron microscope (FEI) equipped with a K3 direct electron detector with a pixel size of 0.33 Å/pix (in super-resolution mode), at a defocus range of -0.5 to -3.0 µm. All movies were dose fractionated into 40 frames. The movies for dataset 1 were recorded with a total dose of 54 e-/$Å^2$, dataset 2 - with a dose of 47 e-/$Å^2$, and for dataset 3 - a dose of 44 e-/$Å^2$.

All data processing was performed in relion 3.0 (*40*). All micrographs were motion corrected using motioncorr 1.2.0 (*41*) and binned two-fold. All micrographs were CTF corrected using Gctf (*42*). Particles were autopicked using templates from manual picking. In total 1692104 particles were picked for data set 1, 1898968 particles for data set 2 and 990286 particles for data set 3. After several rounds of 2D classification, data set 1, 2 and 3 were left with 253789, 1173076 and 741081 particles respectively. 3D Classification with four classes was used to further process each dataset, with C1 and C2 symmetry imposed. The particles from the best classes in each data set were chosen and further refined. The extracellular density for NB4 was masked out for all subsequent refinements to generate refined 3D maps at a resolution of 4.37 Å (dataset 1), 4.25 Å (dataset 2) and 4.61 Å (dataset 3) in C2 symmetry. The particles were merged into a single selection and subjected to refinement, ctf refinement and particle polishing, yielding a final refined map of 3.57 Å resolution (C2 symmetry). The same particle selection produced a reconstruction at 3.83 Å resolution without symmetry imposed (C1). Model building was performed in coot (*43*). The model was refined using phenix.real_space_refine in Phenix (*44*). For model validation the model atoms were randomly displaced (0.5 Å), and the resulting model refined using one of the refined half maps (half-map1). Map vs model FSC was calculated using the model against the corresponding half-map1 used for refinement, and for the same model versus the half-map2 (not used in refinement) (*45*). Model geometry was assessed using MolProbity (*46*).

Protein crystallization, X-ray data collection, processing and structure determination

Crystallization of Cya-SOL-NB4 complex was performed using standard vapour diffusion techniques at 20°C. Concentrated protein complex was prepared by mixing purified Rv1625c and NB4 in 1:1.2 ratio in a buffer of the following composition: 20 mM Tris-HCl pH 7.5, 150 mM NaCl, 5 mM $MnCl_2$ and 1 mM MANT-GTP. This protein solution was used to set up 96-well sitting drop crystallization trials using TPP Mosquito LCP robot. Formulatrix Rockimager was used to visualize crystal formation. Multiple crystal hits were obtained, and selected conditions were used as starting points for further

crystal optimizations. The optimal crystals were obtained after mixing 1.5 µl of protein (20 mg/ml) with 1.5 µl of reservoir solution (0.1 M Na-acetate pH 5.5, 0.02 M $CaCl_2$, 30% MPD). The crystals were gently transferred to cryoprotectant consisting of 0.05 M Na-acetate pH 5.5, 0.01 M $CaCl_2$, 35% MPD, and crystals were subsequently mounted onto crystal loop (Hampton Research) and flash frozen in liquid nitrogen.

X-ray data collection was performed at the PXI and PXIII beamlines at the Swiss Light Source synchrotron in Villigen, Switzerland. The best dataset was collected to 1.97 Å resolution from a single crystal at cryogenic temperature (100 K) using Eiger detector with oscillation range of 0.1°. The data was processed using MOSFLM and XDS (*47, 48*). The resolution cutoff was chosen taking into account the values of CC1/2 and mean I/sigma(I) (*49*). Phasing/refinement was performed using Phenix (*44*). Phases were resolved by molecular replacement (MR) using templates (cya: 5O5K, nanobody: 6FPV). Coot was used for model building and geometrical optimization (*43*). Crystallographic data collection and refinement statistics are shown in Table S2.

Molecular dynamics (MD) simulations

The MD simulations were performed using CHARMM36m force field in GROMACS 2019.3 (*50*). The missing N- and C-terminus of Cya were modelled using I-TASSER server (*51*), and the protein was inserted into lipid membrane, solvated and ionized using the Membrane Builder tools in CHARMM-GUI (*52*). Lipid membrane composed of 60 POPC, 40 POPG, 40 POPE, 20 POPI, 20 DLGL and 20 cholesterol molecules. The system was solvated with TIP3 water molecules extended to 25 Å from the edge of the protein and with per lipid hydration number of 50. Subsequently the system was neutralized with Cl^- ions, and then was brought to a final concentration of 0.15 M KCl or 0.15 M $MgCl_2$. All of the generated systems were subjected to energy minimization, and 6-step NVT and NPT equilibration using the default scheme provided in the CHARM-GUI (3), followed by 200 ns of a production run. Final trajectories were analyzed using tools in available the GROMACS package. The Volmap tool in VMD (*53*) was used for generating occupancy/density maps. The figures related to the MD simulations were prepared using VMD or Pymol.

Limited proteolysis-coupled mass spectrometry

Wild-type and mutant Cya protein preparations were diluted in LiP buffer (1 mM $MgCl_2$, 150 mM KCl, 100 mM HEPES-KOH pH 7.4) with 0.1% digitonin. Mutant and wild-type samples were split into 8 samples each at a protein amount of 2 µg of protein per 50 µL of buffer. Four out of eight WT and mutant samples were treated with proteinase K from *Tritirachium album* (Sigma Aldrich) (limited proteolysis, LiP), whereas the other four were treated with water instead (TC). The samples were incubated in a Thermocycler for 5 minutes at 25°C. Proteinase K was inactivated by heating the samples to 99°C for 5 minutes, then incubating them at 4°C for 5 minutes, followed by the addition of the same volume of 10% sodium deoxycholate. LiP and TC underwent the same procedures.

Tryptic digest. Following the addition of sodium deoxycholate, disulfide bonds were reduced by adding tris(2-carboxyethyl)phosphine to a final concentration of 5 mM and incubating the samples at 37°C for 40 minutes with slight agitation. Free cysteine residues were alkylated with iodoacetamide at a final concentration of 40 mM and 30 minutes of incubation at room temperature in the dark with slight agitation. The samples were diluted with 100 mM ammonium bicarbonate to a final sodium deoxycholate concentration of 1 %. Lysyl endopeptidase LysC was added at an enzyme to substrate ratio of 1:50 and samples were incubated for one hour at 37°C with slight agitation. Next, trypsin was added at an enzyme to substrate ration of 1:50 and incubated at 37°C overnight with slight agitation. The digestion was stopped by adding 50% formic acid to the samples to achieve a final concentration

of 2% formic acid. Precipitated sodium deoxycholate was removed by filtering through a Corning® 2 µM PVDF plate and samples were further desalted on a 96-well MacroSpin plate (The Nest Group). Peptides were eluted with 80% acetonitrile, 1% formic acid and dried in a vacuum centrifuge. After drying, samples were reconstituted in 20 µL 0.1% formic acid and iRT peptides (Biognosys) were added.

LC-MS/MS data acquisition. Samples were measured on an Orbitrap Exploris™ 480 mass spectrometer (Thermo Fisher), equipped with a nanoelectrospray source and an Easy-nLC 1200 nano-flow LC system Thermo Fisher). 1 µL of digest was injected and separated on a 40 cm x 0.75 i.d. column packed in-house with 1.9 µm C18 beads (Dr. Maisch Reprosil-Pur 120) using a linear gradient from 3 to 35 % B (eluent A: 0.1% formic acid, eluent B: 95% acetonitrile, 1% formic acid). Gradient duration was 30 minutes, whereas the whole method was 60 minutes long. Samples were measured at a constant flowrate of 300 nL/min while the column was heated to 50°C. All samples were acquired in DIA (41 windows, 1 m/z overlap) and analyzed in Spectronaut v15 (Biognosys). Further data analysis was carried out in R using mainly the R package protti (*54*). Briefly, the abundances of Rv1625c mutant and wild type where compared in the tryptic controls and the protein abundances in the LiP-samples were corrected accordingly. Statistical testing on peptide level to detect peptide abundance differences was conducted employing the proDA (*55*) algorithm, implemented in protti. The Rv1625c PDB file was edited and the b-factors were replaced with the maximum absolute value of the calculated $\log_2$(fold change) at each position. In pyMOL the protein was then colored according to the replaced b-factors to highlight regions changing regions.

LiP-MS data interpretation. Whether a peptide decreases or increases in abundance is dependent on the accessibility of the native protein to PK. In a standard LiP-MS experiment, three peptide types can be detected, dependent on the proteolytic cleavage:

- Semi-tryptic peptides are generated by a cleavage of PK on either the N-terminal or the C-terminal side of the peptide and a cleavage by trypsin on the respective other side.
- Tryptic peptides are not cleaved by PK at all.
- Non-tryptic peptides were cleaved by PK on both sides.

Depending on the peptide type an increase or decrease in abundance can be interpreted in different ways. A tryptic peptide that decreases in abundance was additionally cleaved by PK, hence it disappears. This likely means that the protein region became more accessible to PK. On the other hand, a tryptic peptide that decreases in abundance can be interpreted as the region becoming less accessible to PK. A semi-tryptic peptide that increases in abundance can be explained as the protein region cleaved by PK becoming more accessible. A semi-tryptic peptide that decreases in abundance can be explained in two different ways: either the protein region became more protected, hence inaccessible to PK, or the protein region became more accessible and the peptide was not detected because of additional PK cleavage sites that were introduced with the conformational change.

Supplementary Figures

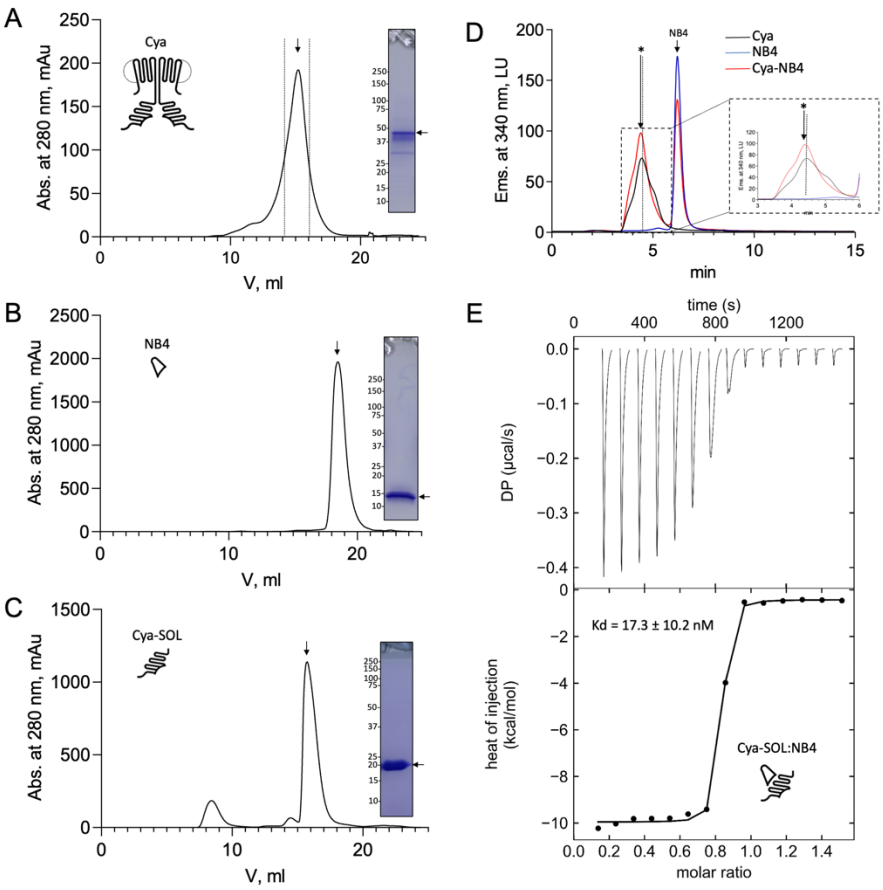

Figure S1. Purification and characterization of Cya. (A) Size-exclusion chromatography (SEC) and SDS PAGE of the purified Cya. SEC was peformed using a Superose 6 Increase column. **(B-C)** Same as in A, for NB4 (B) and for Cya-SOL. SEC was performed using a Superdex 200 Increase column. **(D)** Analytical SEC analysis Cya-NB4 interaction was performed using the Agilent Bio SEC-5 column. The shift of the SEC peak upon NB4 binding is indicated with an arrow; a dashed line indicates the position of the Cya alone. **(E)** Isothermal titration calorimetry (ITC) analysis of Cya-SOL / NB4 binding; mean K_d ± S.D. is indicated in the graph (n = 3). ITC thermogram integration was carried out using NITPIC. Global analysis of integrated thermograms was performed using SEDPHAT and figures were generated using GUSSI.

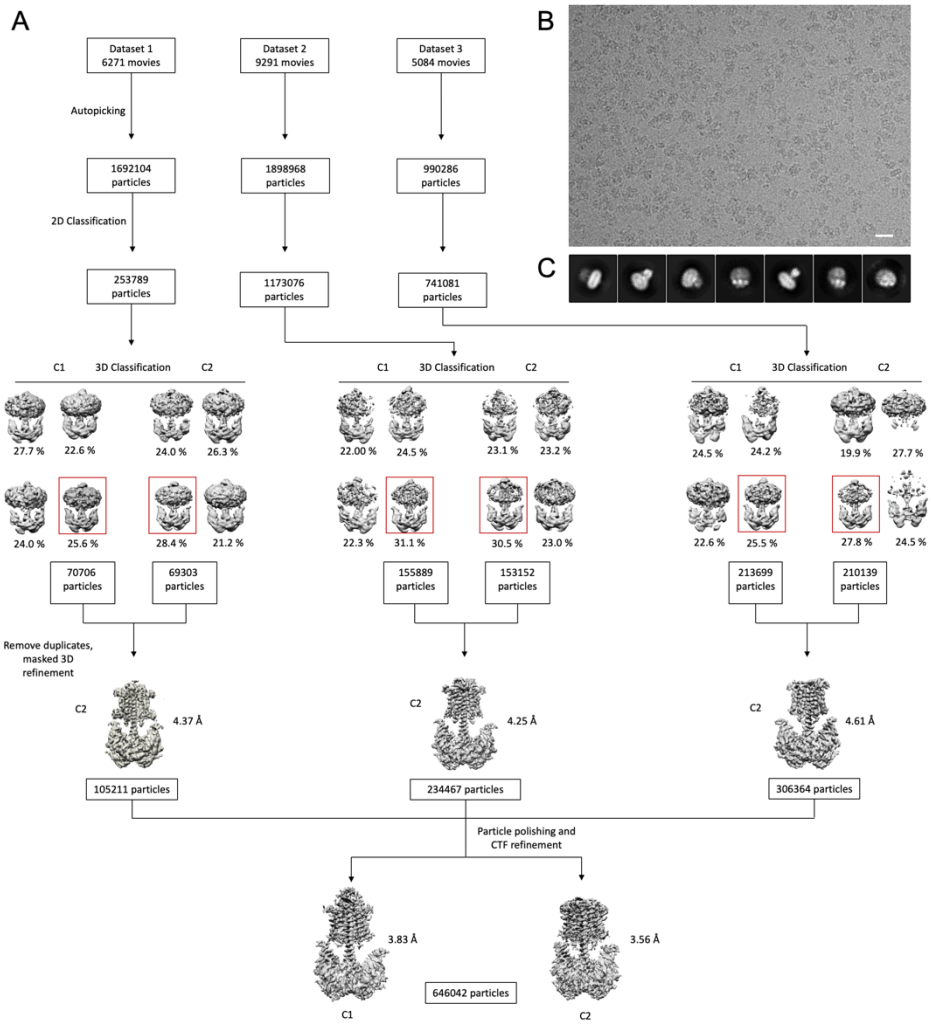

Figure S2. Cryo-EM processing workflow. (A) A processing pipeline for 3D reconstruction of the Cya-NB4 complex. Three data sets were processed in both C1 and C2 symmtery in parallel. Particles resulting from the best 3D classes were pooled, duplicates removed, and the resulting particle selection was refined in C2 symmetry for each data set. All three datasets were combined and further processed by particle polishing and CTF refinement, resulting in two density maps: one processed in C1 symmetry (at a resolution of 3.83 Å) and another one in C2 symmtery (at a resolution of 3.57 Å), as detailed in "Materials and Methods". **(B)** An example of a cryo-EM micrograph the bar corresponds to 200 Å. **(C)** Representative 2D classes reveal distinct views of the Cya-NB4 complex.

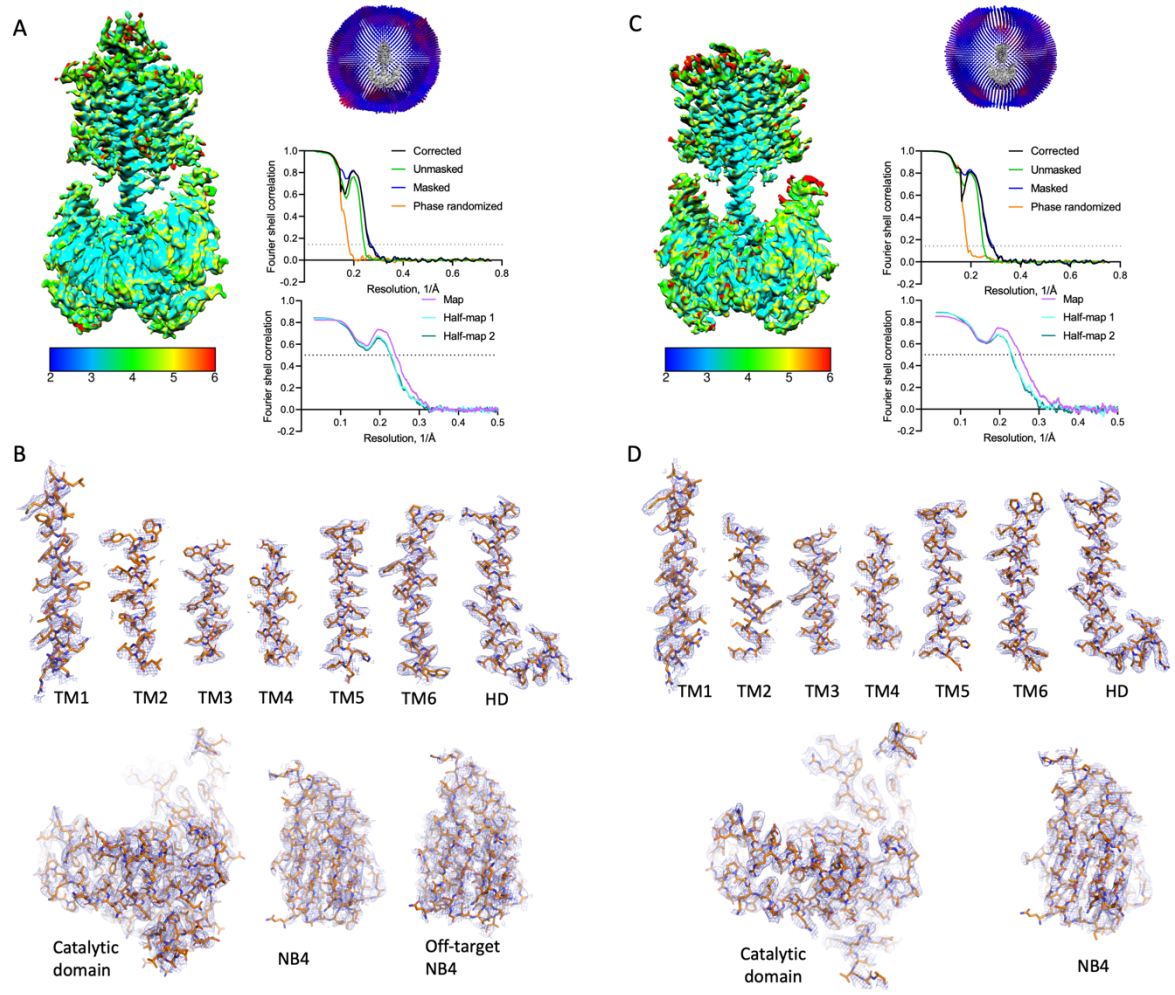

Figure S3. Properties of the Cya-NB4 density maps. (A) Local resolution, angular distribution and FSC curve of the Cya-NB4 complex processed in C1 symmetry. Scale bar indicates local resolution range in Å. **(B)** Isolated cryo-EM density for each of TM helix and the HD contoured at 8σ (*top*). Isolated Cryo-EM density for catalytic domain and NB4 contoured at 8σ, with extracellular NB4 contoured with 4σ (*bottom*). **(C-D)** Same as A-B, for the Cya-NB4 processed in C2 symmetry. All density map features are contoured at 8σ.

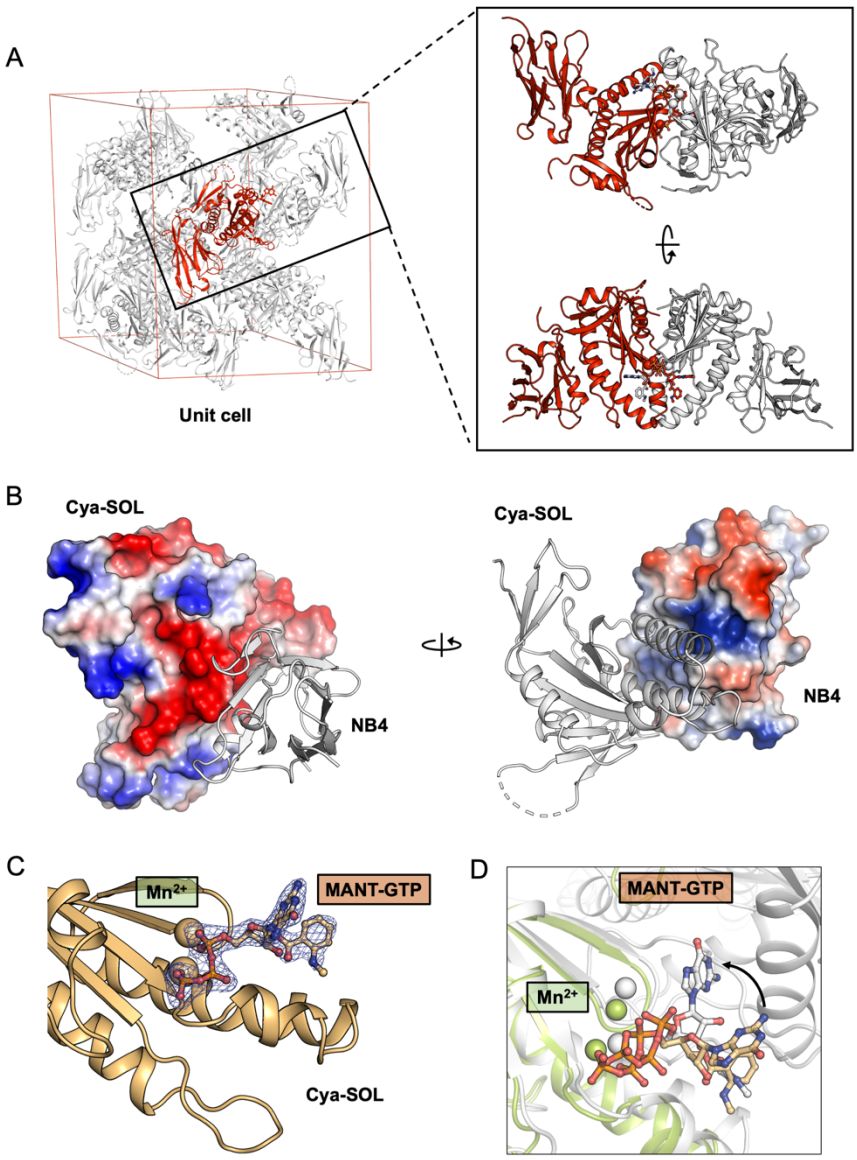

Figure S4. X-ray structure of the catalytic domain of Cya, Cya-SOL, bound to NB4. (A) Illustration of a crystallographic unit cell in the crystals of catalytic domain of Cya-NB4 complex showing the arrangement of one copy of Cya-SOL-NB4 complex (red) in an asymmetric unit (red). Analysis of the interaction between Cya-SOL-NB4 with its symmetry mates (grey) shows that Cya-SOL-NB4 does engages in non-native interactions with its neighbours, consistent with formation of a crystallographic dimer (*right*). **(B)** The surface representations of the catalytic domain of Cya (*right*) and NB4 (*left*), coloured according to the calculated electrostatic potential, suggest a role of the surface-exposed charged residues in the Cya-NB4 interaction. **(C)** Fo-Fc omit map of MANT-GTP (*left*) bound to Cya-SOL. Density is contoured at 3σ, carved to 1.6 Angstrom in Pymol. **(D)** Despite retaining the ability to bind the MANT-GTP molecule via one-half of its catalytic site, the position of the nucleotide is distinct from that observed in the structure of the nucleotide-bound dimeric Cya.

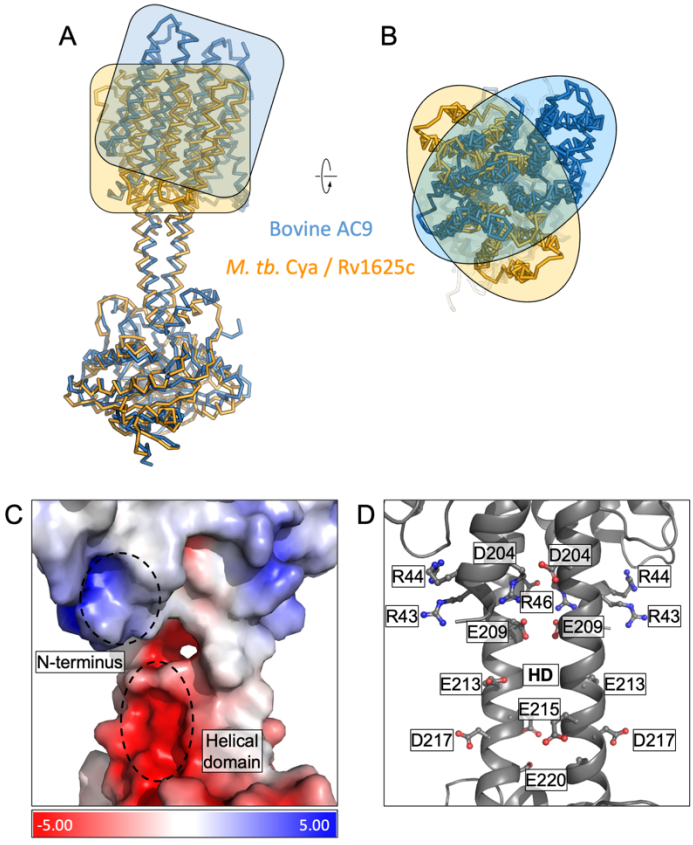

Figure S5. Comparison of *M. tuberculosis* Cya and bovine AC9. (A) Structural alignment of Cya and bovine AC9 using their catalytic domains. The TM regions show considerable deviation in alignment, highlighted by orange/blue boxes (*left*) and ovals (*right*) outlining the protein shapes. The top view of the alignment shows an approx. 90˚ rotation of the bAC9 TM domain compared to that of Rv1625c further highlighting the global structural difference between the two cyclases. **(A-B)** Vacuum electrostatic charge distribution of the N-terminus and the HD of Cya **(C)**. The positively charge residues of the N-terminus may interact with the negatively charged residues of the HD **(C-D)**.

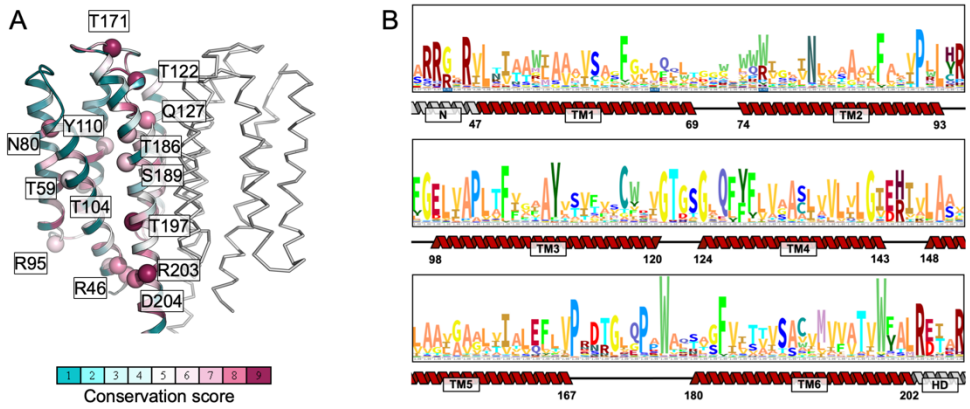

Figure S6. Sequence conservation of the transmembrane domain residues of mycobacterial Cya homologues. (A) The conservation scores were calculated using ConSurf *(56)*, using multiple sequence alignment including 170 homologues of Cya from mycobacteria; the sequences of the homologues were obtained by a Blast search. **(B)** The HMM logo of the aligned sequences used in the ConSurf analysis. The secondary structure features indicate the relative positions of the residues in the TM domain.

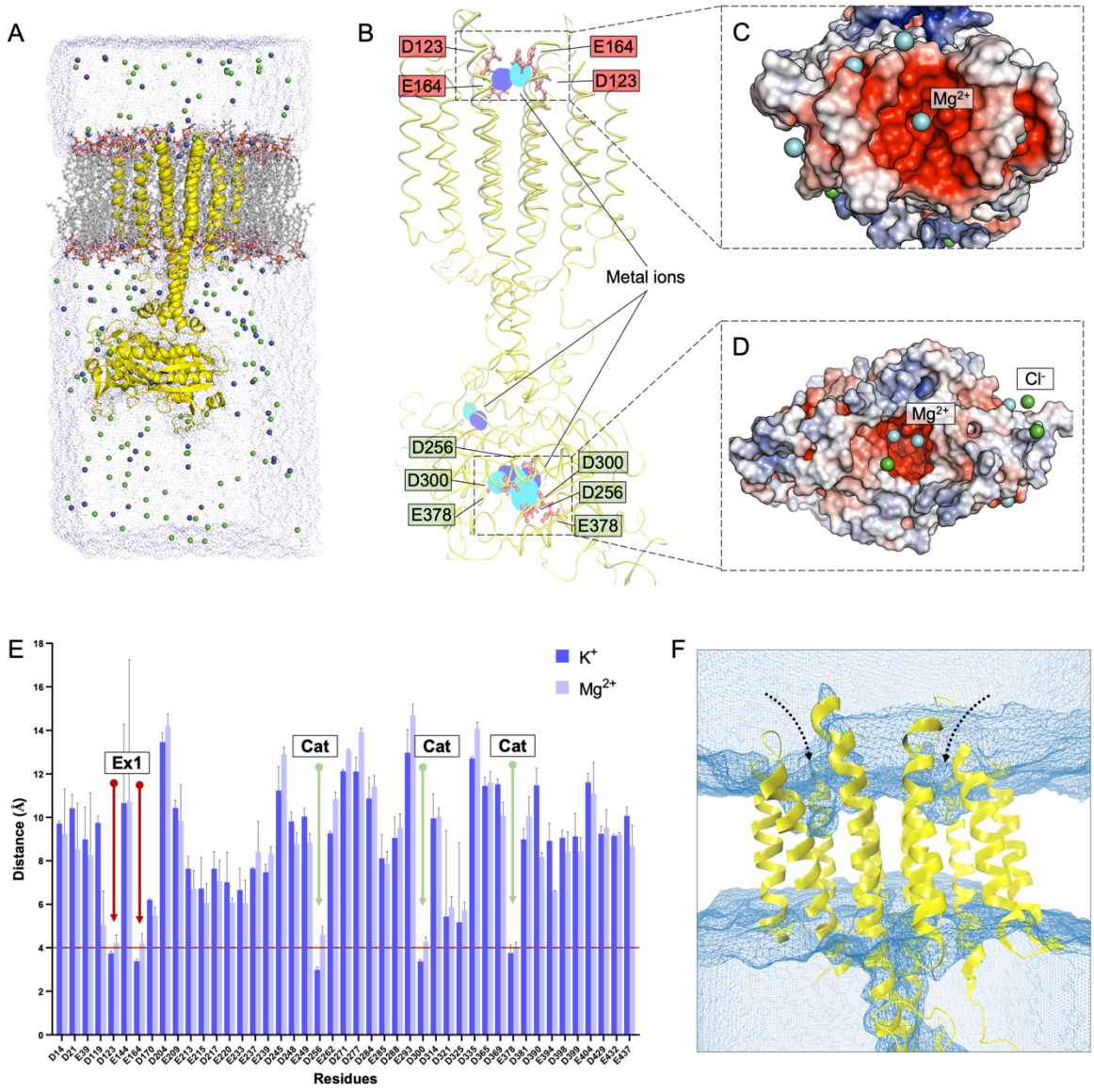

Figure S7. **Molecular dynamics simulations of Cya. (A)** Illustration of Cya embedded in lipid bilayer, solvated with TIP3 water molecules and neutralized with 0.15 M KCl or $MgCl_2$ for molecular dynamics (MD) simulations. **(B)** Overlay of potassium (blue) and magnesium (cyan) occupancy maps from independent simulations fitter on the reference structure (yellow). **(C, D)** Depiction of Mg^{2+} and Cl^- ions present within 4 Å of Ex1 site and of the catalytic pocket of Cya at the end of a 200 ns simulation. **(E)** Average distances between negatively charged residues and K^+ (light blue) or Mg^{2+} ions (cyan) during the course of a simulation. **(F)** The density grid of water molecules (blue mesh) showing the partial solvent accessibility of Ex2 pocket during simulation.

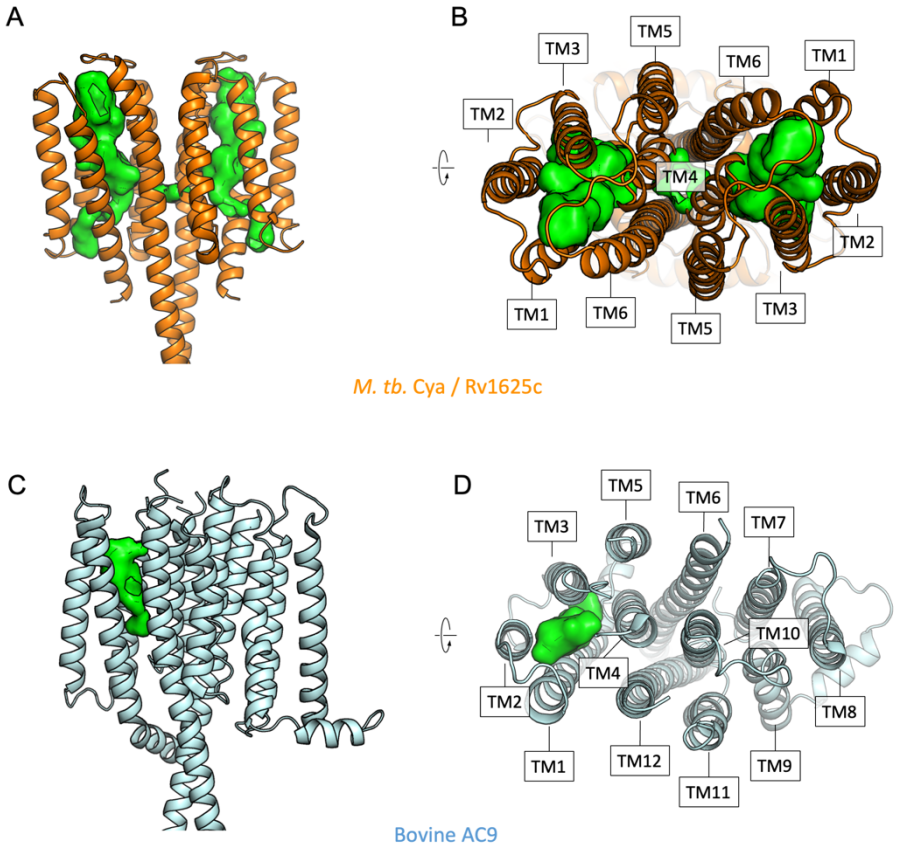

Figure S8. Comparison of the intramembrane cavities formed by Cya and AC9. (A) A side view of Cya (light orange) with the Ex2 cavity (bright green) depicted with a cavity detection of 2.5 Å solvent radius and a cavity detection cutoff of 4 Å solvent radius (*left*). The cavity is discontinuous due to stearic constriction, yet prominent and could potentially accommodate a sufficiently small molecule. (*right*). **(B)** A view of the Ex2 cavity perpendicular to the plane of the membrane. The cavity is formed by TM helices 1, 2, 3, 4 and 6. **(C-D)** Same as A-B, for bovine AC9 (light blue) The cavity in bAC9 is less prominent but located in a similar position. However, any potential structural changes could cause the cavity to open (*right*). The cavity in bAC9 is formed by TM helix 1, 2, 3 and 4 (D).

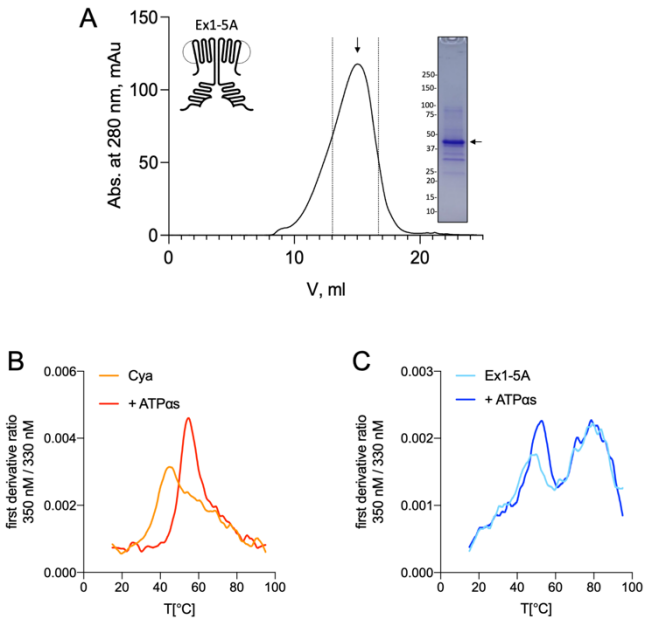

Figure S9. Purification and stability of Cya mutant Ex1-5A. (A) Size exclusion chromatography (SEC) and SDS PAGE of Ex1-5A. The dashed lines indicate the selected fractions of the purified protein sample. **(B)** Analysis of protein thermostability, performed using Prometheus Panta instrument, shows that wild-type Cya has an apparent melting temperature of ~42˚C, and is stabilized by addition of the nucleotide analogue (ATPαS), resulting in the shift of the first derivative ratio (350 nm / 330 nm) peak towards higher temperatures. Here, a representative experiment is shown (the average T_m values are shown in Fig. 5). **(C)** Same as in B, for Ex1-5A mutant. The mutant displays a different melting profile, with additional peaks appearing in the high temperature range. Addition of ATPαS shifts the first peak towards high temperatures.

Table S1. Cryo-EM analysis and statistics

Instrument	FEI Titan Krios / Gatan K3 / GIF Quantum LS	
Magnification	130000x	
Voltage (kV)	300	
Electron Dose (e-/Å2)		
Dataset 1	54 e-/Å^2	
Dataset 2	47 e-/Å^2	
Dataset 3	44 e-/Å^2	
Defocus range (μm)	-0.5 to -3.0	
Pixel size (Å)	0.66	
Refinement		
Number of particles	646042	
Map symmtery	**C2**	**C1**
Map FSC, 0.143	3.57	3.83
Map sharpening b-factor (Å)	-152.693	-155.051
Model to map FSC, 0.5	3.89	4.12
Map CC (mask)	0.69	0.66
Model composition, atoms (hydrogen atoms)	15172 (7558)	16917 (8413)
Protein residues/ligands	990/6	1107/6
Bond length, R.M.S.D.	0.003	0.01
Bond angle, R.M.S.D.	0.663	1.830
Validation		
MolProbity score	1.44	3.03
Clash score	8.17	26.19
Rotamer outliers (%)	0.77	10.59
Mean B-factors protein / ligand	45.09 / 39.85	92.01 / 77.95
Ramachandran plot		
Favoured (%)	98.36	95.06
Allowed (%)	1.23	4.39
Outliers (%)	0.41	0.55

Table S2. X-ray data analysis and statistics

	Rv1625c(sol)-NB4
Wavelength	0.999879
Resolution range	47.4 - 1.973 (2.044 - 1.973)
Space group	P 65 2 2
Unit cell	94.793 94.793 119.655 90 90 120
Total reflections	774280 (34068)
Unique reflections	21585 (1492)
Multiplicity	35.9 (22.8)
Completeness (%)	93.96 (66.85)
Mean I/sigma (I)	25.4 (1.5)
Wilson B-factor	44.58
R-merge	0.090 (1.587)
CC1/2	1.0 (0.685)
Reflections used in refinement	21584 (1492)
Reflections used for R-free	1077 (75)
R-work	0.2061 (0.3126)
R-free	0.2443 (0.3728)
Number of non-hydrogen atoms	2539
Macromolecules	2325
Ligands	57
Solvent	157
Protein residues	299
RMS(bonds)	0.004
RMS(angles)	0.83
Ramachandran favored (%)	98.28
Ramachandran allowed (%)	1.38
Ramachandran outliers (%)	0.34
Rotamer outliers (%)	2.85
Clashscore	8.31
Average B-factor	57.91
Macromolecules	57.29
Ligands	62.31
Solvent	65.52